WILEY

IET-Wiley Virtual Symposium on Renewable Energy 2022

Digital and flexible control and operation of transmission and distribution grids for renewable power systems.

September 13 2022

Research conducted at institutions in Germany has led to exciting advances in the areas of renewable energy. This free virtual symposium supported by two of the IET's flagship open access journals *IET Renewable Power Generation (RPG)* and *IET Generation, Transmission & Distribution (GTD)* will be free to attend. It will provide a forum for researchers based in Germany to highlight their research and will celebrate the capacity for renewable energy research to engineer a better world.

Session Topics Include:

- Power Flow Control for efficient Transmission Grids
- Digitalization of Power Systems
- Flexibility in Power Systems
- Smart Distribution Grids

Register free today

The Institution of Engineering and Technology

Received: 24 September 2021 | Revised: 9 February 2022 | Accepted: 28 March 2022

IET Generation, Transmission & Distribution

DOI: 10.1049/gtd2.12486

The Institution of Engineering and Technology WILEY

ORIGINAL RESEARCH

Experimental verification of smart grid control functions on international grids using a real-time simulator

Rajkumar Palaniappan[1] | Oleksii Molodchyk[1] | Mahdi Shariati-Sarcheshmeh[2] | Marilyn Winifred Asmah[1] | Jiayan Liu[1] | Tobias Schlichtherle[3] | Frank Richter[3] | Ekow Appiah Kwofie[4] | Daniel Rios Festner[5] | Gerardo Blanco[5] | Anna Mutule[6] | Olegs Borscevskis[7] | Shady S. Rafaat[8] | Yong Li[9] | Ulf Häger[1] | Christian Rehtanz[1]

[1]Institute ie[3], TU Dortmund University, Dortmund, Germany

[2]EQOS Energie GmbH, Pfungstadt, Germany

[3]Energie Waldeck-Frankenberg GmbH, Korbach, Germany

[4]West Africa Energy Program, Accra, Ghana

[5]Facultad Politécnica, Universidad Nacional de Asunción, San Lorenzo, Paraguay

[6]Smart Grid Research Centre, Institute of Physical Energetics, Riga, Latvia

[7]Sadales tīkls AS, Riga, Latvia

[8]Texas A&M University, Doha, Qatar

[9]Hunan University, Hunan, China

Correspondence
Rajkumar Palaniappan, Institute ie[3], TU Dortmund University, Figge Str. 70, 44227 Dortmund, Germany.
Email: rajkumar.palaniappan@tu-dortmund.de

Funding information
i-Automate, Grant/Award Number: 03ET7561A; German Federal Ministry for Economic Affairs and Energy (BMWi)

Abstract

The drastic increase in distributed energy resources (DERs) leads to challenges in the operation of distribution systems worldwide. While several solutions for grid monitoring and control are available on the market and in literature, this research is the first of its kind aiming to supervise the grid by providing a modular configurable unified hardware and software architecture. The control algorithms are configured using data models according to IEC 61850-7-3 and IEC 61850-7-4. The novel system architecture is a portable, modular and flexible architecture that aggregates smart grid control functions onto a standardised hardware platform, emphasising the need for hardware independence. The central controller contains several smart grid control functions and the various field devices are distributed across the distribution grid. This paper deals with the simulation of different real-world distribution grids on the Real-Time Simulator (RTS) and experimental verification of the control algorithms. Smart grid control functions such as Coordinated Voltage Control (CVC) and Optimal Power Flow (OPF) are experimentally verified on a German grid. The grid dynamics are compared when the central controller executes the CVC against the OPF implementations. The experimental results, advantages and challenges of each control are presented here. The results also showed the variation in grid behaviour when the control parameters were varied. The paper also shows that the algorithm and the choice of the control parameters depend upon the distribution grid's complexity and the system operator's individual needs. The results illustrate the potential of such a universal distribution automation solution for system operators worldwide.

1 | INTRODUCTION

Distributed energy resources (DERs) are becoming a significant factor in the global trend against climate change around the globe [1]. The renewable energy source (RES) integration has grown the fastest in 2020 in the last two decades and is expected to grow even more in the following years [2]. Germany's initial plan of achieving an electrical grid where renewables provide 40–45% of the total electricity consumption by 2025 was already reached in 2020 [3]. The integration of decentralised, renewable energy sources (RES) into the electrical energy supply grid is often associated with developing intelligent distribution grids (smart grids). With these changes, the passive electrical grids are changing towards active distribution grids (ADGs). Some intelligent grid functions, like wide-area monitoring, are already established in high and extra-high voltage (HV/EHV) levels. However, the protection and control devices in the higher voltage levels are too inflexible and expensive to use in the medium and low voltage (MV/LV) levels. Incorporating these devices directly into the distribution grids would incur inconsiderable operational and financial costs.

The high penetration of these uncertain components has a considerable impact on the power quality of the electrical grid, especially on voltage control. Voltage control is the system operator's responsibility to maintain the voltage within the prescribed limits (as per local regulations). Considering the inherent vulnerabilities, maintaining the voltage within the limits prescribed by [4] is becoming more challenging for the distribution system operators (DSOs). For the present scenario, each DSO can decide either to expand the grid or install intelligent components in their grid, with the help of which they keep the voltage within the prescribed limits. Having said that, the DSOs also have the added responsibility to coordinate with their overlying transmission grid operators (TSOs) to control the reactive power flow, failing which the grid codes will imply vast amounts of monetary fines on the DSOs.

Some innovative methods could solve these inherent challenges of the system operators. One possible solution to address this challenge is the real-time control of the available flexibilities. More field measurements are required in real-time to operate the distribution grid at its full capacity to mitigate challenges such as voltage and thermal violations. Intelligent algorithms will use these measurements to decide which flexibilities to control in order to maintain the voltage within the predefined limits. This automation system at the primary substation should ideally contain intelligent algorithms. It should allow the DSOs to select the control architectures and coordinate between many DERs cost-effectively to control voltages within the grid and minimise RES curtailment.

The research on automation architectures based on such concepts has recently experienced massive growth. Several cloud-based solutions are offered in the industry for grid monitoring [5, 6] using intelligent electronic devices (IEDs) in the grid. However, it involves additional measurement infrastructure in the field and communicating it to the cloud. In terms of software, many developers aim to bring all possible algorithms under one hood to provide analysis tools for efficient control and observability of the power system. However, such a solution requires an enormous investment in terms of measurement installation and the information and communication infrastructure (ICT) infrastructure. Higher-level control functions are already being actively used to operate HV/EHV transmission grids. Moreover, unlike the physical hardware devices, the functional migration to distribution grids is associated with little to no financial burden, making the above-mentioned software tools attractive for smart grid applications.

While numerous researchers work on developing automation systems for smart grids to introduce improvements in terms of communication robustness, performance or security, very little attention is being devoted to the experimental validation of such methods on grids with different topologies and comparison of the implemented control strategies. Only individual functionalities of a smart grid have been implemented and prototypically tested in various research projects until now [7–10]. This research, however, introduces an overall concept

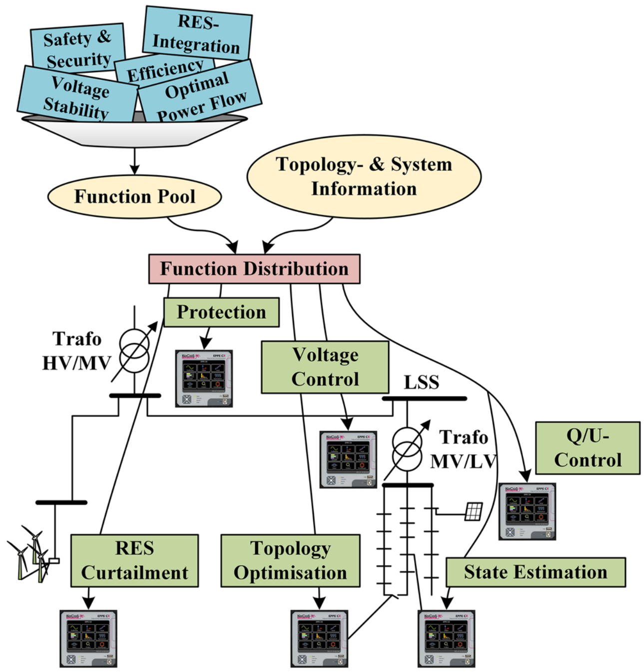

FIGURE 1 Concept of the proposed smart grid automation system

for a modularly configurable and testable automation architecture for smart grids. One of the significant ideas of the proposed research is the separation of software applications from hardware devices. In essence, it means that the software can be device-independent and can be easily ported to another hardware device from another vendor. This is done by configuring the algorithms based on the IEC 61850 data models.

This implementation focuses on decentralised measurements in the distribution grid. Some of the control functions typically implemented at the central controller device at the primary substation are state estimation (SE), Coordinated Voltage Control (CVC) and Optimal Power Flow (OPF). SE processes all measurements to estimate the system state. While the CVC is a standalone application, typically based only on the actual voltage values, the OPF is inspired by MATPOWER [11]. The algorithms are configured based on the data models according to IEC 61850-6, as explained in the author's previous work [12]. Although the original idea was to validate the implemented algorithms in a field test, it was then expanded to experimentally check the validity of the algorithms in different real-world grids. Figure 1 describes the overall concept.

The main contributions of this paper are as follows:

1. The implemented smart grid control functions configured using IEC 61850 data models are presented.
2. Several real-world grids from different countries are simulated on the digital real-time simulator (RTS).
3. The implemented CVC and OPF algorithms are experimentally verified to check which algorithm performs better under grid violations.

The aim is to test the proposed system for real-world grids from six different countries in a hardware-in-the-loop (HiL) setup, where these grids are simulated on the RTS. The representative grids are chosen from project partners from six countries: Australia, China, Germany, Ghana, Latvia, and Paraguay. It has to be mentioned that they are only representative real-world grids and do not exemplify the entirety of the country. For this research, the grids were considered symmetrical. For the sake of anonymity, no names of the grids or locations will be discussed in this paper. The communication and coordination between the RTS and the various IEDs are done using User Datagram Protocol (UDP). In this case, since several measurement points had to be considered, taking into account the complexity of the various grids, all the client IEDs were simulated and only the controller IED was used as explicit hardware during the HiL simulations. Using these simulated grids, the efficiency of the CVC algorithm was compared against that of the OPF algorithm.

The remainder of the paper is structured as follows: Section 2 describes selecting the available control algorithms and the novelty of the presented research. Section 3 explains the implemented control algorithms (CVC, OPF) in detail. Section 4 introduces the six selected test grids and discusses the simulation environment. Section 5 presents the simulation results and compares the efficiency of the implemented algorithms. Finally, Section 6 concludes the paper with an outlook on further research on the topic.

2 | ACTIVE DISTRIBUTION GRID CONTROL

2.1 | Measurement infrastructure in ADGs

Before implementing complex control algorithms, one must establish a robust measurement infrastructure. The fact that the electrical grid is neither connected in terms of ICT infrastructure nor has any automation can increasingly pose a problem for the DSO. With the increasing integration of DERs, new loads such as electric vehicles, and storage systems into the MV/LV grids, conventional operations as before can jeopardise the system stability of the distribution grid. In the modern distribution grids, almost all HV/MV substations are equipped with On-Load Tap Changers (OLTCs), which can also be tapped remotely.

In radial MV grids with little to no DER penetration, voltage drops along the feeders, which means that the highest voltage is typically at the substation, making it suitable for the voltage measurement and the subsequent adjustment of the OLTC tap setting. Many DSOs use the secondary-side voltage or current at the OLTC as a reference. However, once the DERs are involved, the voltage profile becomes much more unpredictable. Since each DER raises the voltage at its connection point, the nodes of maximum and minimum voltage or the directions of power flows can no longer be identified. In addition, there are also unpredictable loads, such as Electric Vehicles (EVs) and Battery Energy Storage Systems (BESS), leading to the need for ICT infrastructure and a state estimator to determine the system state. These are the essential factors differentiating ADGs from conventional distribution grids.

The author's previous work in [13] deals with an experiment to depict the importance of such decentralised measurements. The paper compared the centralised control using field measurements against a simulation with no field measurements. The results show that even when the OLTC secondary voltage is within limits, the voltages at the branch ends violate the voltage limits. This proved the requirement of decentralised field measurements, especially in an unpredictable environment with lots of RESs.

2.2 | The novelty of the presented research

In addition to the predominantly local autonomous protection and control functions known today, a system architecture must enable higher-level, aggregated and coordinated smart grid automation functions for grid monitoring and control in a flexibly expandable manner. Therefore, an innovative and open architecture should be designed to make it possible to implement grid automation functions that meet the current requirements and, at the same time, make them more adaptable to future conditions in the sense of future-proofing the technical system. However, a particular challenge resulting from this newly gained flexibility lies in the functional testability of the system concerning all possible configurations as a basis for certification for actual use.

The research develops a flexible, configurable and testable automation architecture for smart grids. Among other things, it expands the architectural approach for smart grid functions and designs procedures for automated and comprehensive testing of the proposed novel system solution. The main idea behind this solution is to separate software from hardware and make the functionalities modular. The core part of the project is a program developed in C++, which contains multiple grid functions, such as power flow, SE, time overcurrent protection, distance protection, CVC, OPF etc. A proven and robust hardware and software system from the field of measured value acquisition, power quality analysis and fault recording from the project partner KoCoS serves as the system platform for function implementation [14]. The program and the configuration files of the selected functions are deployed onto the IED. The user is expected to load the grid measurement and communication data model, where the different functions are assigned to the IEDs. The program configures these functions by reading the data model file during the execution.

2.3 | Possible control algorithms

The automation architecture designed in this research focuses on MV/LV automation, thereby enabling the transformation of the conventional grid to an ADG. The control algorithms are supposed to set active power (P) and reactive power (Q) setpoints for the DERs in the grid to remedy voltage limit violations or, in some cases, thermal overcurrents. The different kinds of voltage control techniques are mentioned in [15]. Other DER control methods include local, decentralised, distributed and centralised control based on the ICT infrastructure and the chosen control [16]. While every control method has its advantages and challenges, selecting the proper control methodology according to the selected application is the primary task in voltage control.

One of the simplest methods is local control, that is, the uncoordinated operation of DERs. The idea is that the DERs perform $Q(V)$ control at each node using a linear $Q(V)$ curve, where Q is injected if $V < 1$ p.u. and absorbed if $V > 1$ p.u. Despite this control scheme being relatively simple in its implementation and not requiring high amounts of computational power [17], it does not consider the efficient use of the available flexibilities. To complement the local and central control methods, the decentralised and distributed schemes are presented in [18], where the decisions are made by zonal controllers or communication within different agents. While some works deal with a two-level control scheme [19], others deal with a hierarchical control scheme [20, 21], where the control is switched between local and distributed control.

The proposed implementation considers the centralised control architecture since centralised control offers the best possible system states due to the possibility to control the flexibilities in real-time [22, 23]. Notwithstanding, the centralised control approach has high investment costs, especially from the measurement equipment involved. Since this work involves installing several decentralised measurement devices across the distribution grid, the centralised option is the most optimum for this scenario. However, it has to be said that there is a limitation on the number of measurement devices to be installed in the field. In this case, a grid reduction is made using the Thevenin equivalent [24]. In this way, replacement loads are created and an optimum trade-off is reached between the number of measurement devices and the number of nodes considered to be compensated by the replacement nodes.

The flexibilities considered in this work are the OLTC and P, Q control of the DERs. Potentially, the option of grid reconfiguration could also be considered for thermal overloading. Multiple research works show the importance of meshed operation of the distribution grids, such as reduced line losses and increased RES penetration in the distribution grids [25, 26]. Although this work does not consider a dynamic reconfiguration, such dynamic changes could have devastating effects on system stability, especially in the distribution grids. Also, the adaptation of protection schemes for the changed topology has to be taken into consideration. For these reasons, the dynamic reconfiguration of the distribution grid as flexibility is not considered in this implementation.

The CVC algorithm is a pragmatic and flexible approach to dealing with the voltage violation problem. Instead of controlling the voltages of all nodes at all times, the algorithm utilises the measurement infrastructure and uses the system state from the SE algorithm. From the estimated nodal voltages, the CVC algorithm identifies the minimum and maximum voltages in the grid. Then, in case of a voltage violation at any node in the grid, the algorithm issues user-defined actions such as the OLTC stepping or Q control of DERs. Such a pragmatic solution is also easy to be understood by the DSOs to dynamically change the operating parameters based on the actual system requirement. Another option to maximise the advantage of coordinated DER operation is to apply the OPF algorithm. This solves an optimisation problem where an objective function, subject to constraints, is minimised (or maximised). Since the optimisation is user-defined, this function reflects the control objective, for example, loss minimisation, control costs minimisation, the power drawn from the HV grid, etc. The constraints include the power balance equations in order to respect the grid behaviour. The exact configuration of both CVC and OPF is given in Section 3. An additional possibility is model predictive control (MPC). This algorithm predicts system dynamics by solving an optimisation problem in a receding horizon manner. Its explanation would be cumbersome within this paper's scope and not the main focus. However, it is still worth mentioning as another variant under implementation.

3 | IMPLEMENTED CONTROL ALGORITHMS

As mentioned earlier, although the implementation of any number of control algorithms is possible, this paper focuses only on two: CVC and OPF. For simplicity, the grid is assumed to be symmetric and the calculations are done for a single phase. Based on the measurements from the decentralised devices, the controller device runs the SE algorithm based on the Weighted Least Squares (WLS) method to estimate the system state. This way, all the nodal voltage magnitudes and angles, including the unmeasured ones, can be estimated. The resulting system state is saved for further use by other functions. As a dynamic simulation is used, the SE algorithm is executed periodically at regular intervals. It has to be mentioned that SE delivers feasible results only if the measurement redundancy η is sufficient, that is, if the following condition is satisfied:

$$\eta = \frac{m}{2n-1} \geq 1. \tag{1}$$

Here, n is the number of nodes in the grid and m is the number of measurements (e.g., voltage magnitudes, P, Q). As already explained, the CVC and OPF algorithms use the estimated system state as inputs for their algorithms. When activated, these functions are executed periodically after the SE. The data model implementation helps other functions to identify the current status of the SE algorithm. When idle, both CVC and OPF first check if the minimal time since the last execution has elapsed, after which the SE status is acquired. If SE is currently running,

TABLE 1 Decision table for the CVC algorithm

V_{min} \ V_{max}	V ≤ 0.93	0.93 < V < 0.96	0.96 < V < 0.98	0.98 < V < 1.02	1.02 < V < 1.04	1.04 < V < 1.08	V ≥1.08
V ≤ 0.93	Step up	Step up	Step up	Step up	Q_i control	Q_i control	Q_i control
0.93 < V < 0.96	–	Q_i control	Q_i control	Q_i control	Q_i control	Q_i control	Q_i control
0.96 < V < 0.98	–	–	No control	No control	No control	Q_i control	Q_i control
0.98 < V < 1.02	–	–	–	No control	No control	Q_i control	Step down
1.02 < V < 1.04	–	–	–	–	No control	Q_i control	Step down
1.04 < V < 1.08	–	–	–	–	–	Q_i control	Step down
V ≥1.08	–	–	–	–	–	–	Step down

the functions wait for the completion of the SE algorithm. If SE is already completed, the results of the SE are taken into account as input.

3.1 | CVC

As mentioned in Section 2, CVC first identifies the minimum voltage V_{min} and maximum voltage magnitude V_{max} from all the estimated system states. Although the stipulated limit for maintaining the voltage is ±10%, a safety limit is chosen here as ±7%. In this way, it can be ensured that the system voltage will not violate the specified limits at any point. More information about the CVC control strategy implementation is explained in the author's previous work [13]. The implemented configuration constitutes the following control actions:

- If $V_{min} \leq 0.93$ p.u., $V_{max} \leq 1.02$ p.u. → OLTC step up
- If $V_{min} \geq 0.98$ p.u., $V_{max} \geq 1.07$ p.u.→OLTC step down
- If $V_{min} > 0.96$ p.u., $V_{max} < 1.04$ p.u. → no control
- In all other cases: perform Proportional Integral Derivative (PID) control of the controllable DERs

In this configuration, the proportional K_p, integral K_i, and differential K_d coefficients are decided in a trial and error fashion. The implemented control strategy is depicted in Table 1, which does not include the PID control ranges.

A state flow diagram for the CVC algorithm is shown in Figure 2.

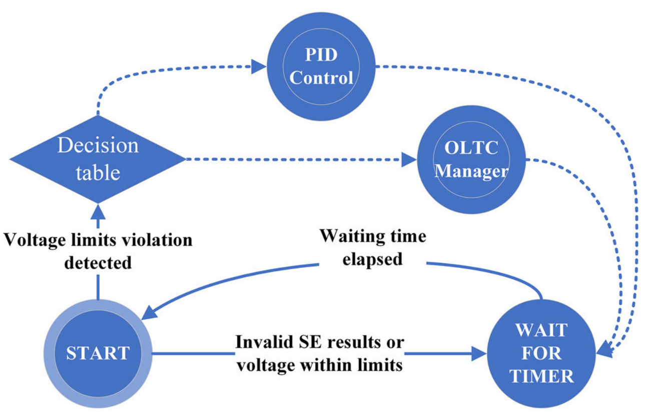

FIGURE 2 CVC implementation at the controller device

3.2 | OPF

The implemented OPF algorithm periodically solves the AC OPF optimisation problem to find the most cost-efficient P, Q setpoints for the controllable DERs. A similar centralised OPF scheme is discussed in [27]. The decision variable in the vector X contains the voltages and angles of all nodes in the system, as well as the P, Q setpoints. The cost function to be minimised is expressed in the following formula:

$$f(X) = \sum_{i=1}^{n_g} \left(c_P \left(\frac{P_{gen,i} - P_{gen,i}^{available}}{MW} \right)^2 + c_Q \left(\frac{Q_{gen,i} - Q_{gen,i}^{previous}}{MVAr} \right)^2 \right). \tag{2}$$

Here, n_g is the number of flexible DERs, $P_{gen,\,i}$ and $Q_{gen,\,i}$ are the P, Q setpoints of the i-th DER, respectively. $P_{gen,i}^{available}$ denotes the maximum available actual P output and $Q_{gen,i}^{previous}$ denotes the Q setpoint set by the previous OPF execution. The coefficients c_P and c_Q are set such that $c_P \gg c_Q$ because Q is to have higher priority since the active power curtailment (APC) would result in higher operational costs for the DSO. The c_Q term forces the Q setpoints to stay as constant as possible to minimise the electrical wear of the inverters. The implementation of the OPF is explained in Figure 3.

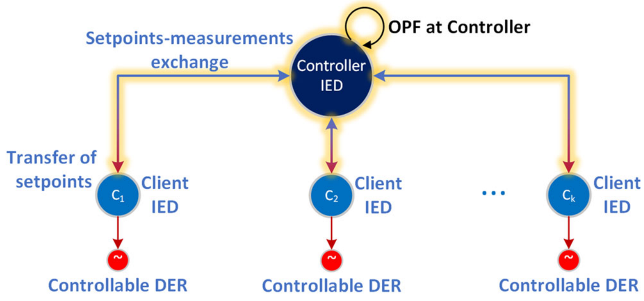

FIGURE 3 Functional working of an OPF algorithm

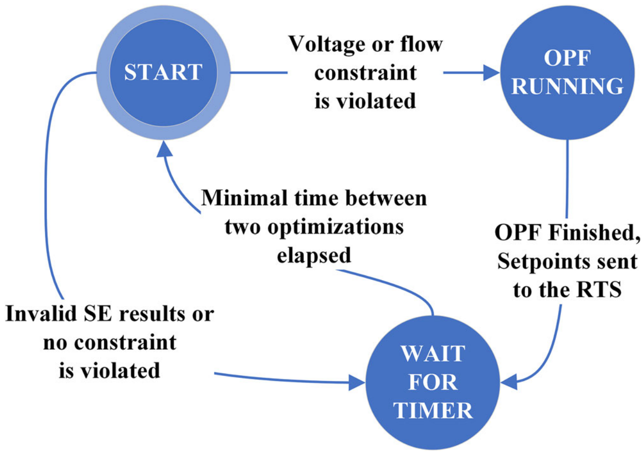

FIGURE 4 OPF implementation at the controller device

A state flow diagram for the OPF algorithm at the controller device is presented here in Figure 4.

The optimisation problem is solved using MATPOWER Interior Point Solver (MIPS) [11]. The solver is manually converted from Matlab into C++ and modified for the application. More information about the OPF control parameters and the constraints are explained in the author's previous work [28]. The constraints to which f(X) is subjected to, are chosen to be:

- Power balance equations to respect the grid behaviour
- Voltage limits of 0.96 p.u. and 1.04 p.u. for minimum and maximum voltage magnitudes, respectively
- Thermal current constraints for each line
- Power factor constraints for inverters setting the lower bound on power factor at 0.9 lag/lead
- The voltage at the slack bus (HV side of substation) is fixed to be 1 p.u. $\angle 0°$ for the optimisation problem to be feasible

The OPF algorithm is called upon only when there is a voltage or a thermal violation. If the grid experiences neither voltage nor current congestions, OPF does not need to be invoked. However, the OPF is always started even if no problems in the grid occur. However, the tap setting of the OLTC is an integer variable and needs to be handled separately since MIPS can only solve continuous optimisation problems. The following algorithm is implemented to include the OLTC as additional flexibility in the solution. First, MIPS starts to compute the grid configuration solution, where the OLTC tap position holds its initial value. If convergence is achieved, the calculated solution is applied. Otherwise, the algorithm changes the current tap setting in its internal grid topology one position higher or lower, depending on the voltage situation, and reruns MIPS. Finally, the tapping is changed as in Equation (3):

$$tap_{new} = tap_{current} \pm one\ tap, \tag{3}$$

In case of convergence, this new solution is accepted. Otherwise, the algorithm assumes that no feasible solution is available and waits until the next time. The experimental verification and the results of the OPF algorithm tested on a Simbench MV grid [29] are available in [28]. The OPF was executed every 30 s, while the estimated states were obtained every 10 s. There is also the option to buffer (the latest three) estimated states and build averages over them to use them as the OPF algorithm.

4 | TEST GRIDS AND SIMULATION SETUP

The international applicability of the implemented control algorithms is crucial since almost all countries are facing the challenge of extensive DER penetration. While the best way to determine the validity of any algorithm is to validate the performance in real-world applications, it is not feasible for all research algorithms to have field tests. For this reason, the implemented algorithms are first tested using software and then using experimental verifications with HiL simulations. When real-world testing is not possible, the HiL simulations are one way of testing the implemented algorithms towards near-world accuracy. In order to validate the implemented algorithms, the grids have to be modelled in the RTS accurately, with all the available DERs specifically parameterised as flexibilities.

Having said that, the parameters of the real-world electrical grids could be completely different from each other. The grid parameters of the international grids may vary extensively, given the geographical location and the historical development of the individual grids. A multitude of factors influences these differences, although not much detail is given to the modelling parameters in this paper.

4.1 | International grid codes

The parameters of the real-world electrical grids could be completely different from each other. For example, the distribution grid characteristics in India could be very different from that of Germany. A multitude of factors influences these variations, although not much detail is given to the parameter differences in this paper. An important factor considering the different real-world grids is the local grid codes and regulations.

The different countries/regions have varying grid codes and regulations regarding voltage quality and CVC control. Multiple works in literature compare the various grid codes and guidelines [30–31], where the prevalent prerequisites and contradictions among the different international standards have been characterised. Several real-world applications and case studies have been investigated in [32–35]. These standards are beneficial for the different DSOs and governmental organisations to evaluate their present status against that of others. It is also helpful for new grid operators to establish new technical requirements from the experience of others who have extensively worked on that. Different organisations (VDE, CENELAC, ENTSO-E) have multiple rules for connecting to the HV, MV, and LV grids, including the ancillary service requirements. These grid codes are also beneficial to learn from the practical challenges, such as the 50.2 Hz problem in Germany, the Low-voltage Ride Through (LVRT) in Spain, the early adoption of Delta control in Denmark or the bundling of resources in the Caribbean or the Pacific islands. It has to be mentioned that the grid codes will constantly be updated to enable and ensure more DER penetration.

In Germany, the standards VDE-AR-N 4110 [36] and VDE-AR-N 4105 [37] describe the connection requirements for the DERs to be connected to the MV and the LV grids. While the international standard IEEE 1547–2018 [38] deals with the connection requirements of DERs to the distribution grid, the European standards are described in [39]. The standards also mandate specific requirements regarding CVC control. The German Federal Ministry for Economic Affairs and Energy (BMWi) mandates that the DERs should, in addition to the monetary benefits for the provision of P, also provide Q to ensure system stability [40].

4.2 | Selected real-world grids

Multiple project partners, colleagues and DSOs from different parts of the world were contacted to acquire representative real-world grids with as many variations as possible. Although many colleagues were interested in the research work, sharing real-world information was not feasible because of data protection reasons. Nevertheless, a few grids were acquired from colleagues and were simulated on the RTS. The representative grids were received from Paraguay, Ghana, Latvia, China and Australia and were selected for this implementation. It also formed a good geographical distribution of the electrical grids worldwide.

Comparing these five representative electrical grids with that of Germany threw a lot of light into understanding the electrical parameters of the grids. However, due to the same data protection reasons, no details about the grids will be mentioned in this paper and all details will be anonymised. A geographical representation of the locations of the grids under test is given in Figure 5. When the electrical parameters are compared against each other, there is a good mixture of the characteristics, and the comparison is shown in Table 2.

FIGURE 5 Representation of the chosen grid locations [41]

The availability and the importance of the DERs and loads are taken into consideration during the selection of the measurement nodes. Since it is not feasible to place measurement devices at many places in the overall grid to achieve full observability, specific nodes are chosen for measurement placement. The measurement locations are marked in green and the nodes with DERs are marked in blue. Unfortunately, the presence and availability of DERs or other flexibilities in the representative grids are lesser than expected. The nodes are also combined with a Thevenin-equivalent algorithm and replacement loads are formed. This reduces the number of nodes in the grid and maintains the observability criterion. In all cases, the central controller is located at the primary substation and the different decentralized measurement devices communicate with the controller at regular intervals. In addition to the transfer of measurements, each client device can perform protection functions by itself. Figures 6–11 illustrate the grid topologies and the RES locations of the different representative grids.

This implementation does not consider support from the transmission grid and only the connection point of the HV/MV grids (substations). For the German grid, real-world data was available. However, there were no voltage violations when the actual measurements were used. For this reason, standard load and generation profiles were selected. There was no data available for the grids from other countries, and standard profiles were the only choice. While all the representative grids had a star or open-ring topology, the German representative grid had a closed-ring topology. This provides a multitude of possible grid topologies and enables the implemented algorithms to be experimentally verified in various grid topologies. It is also interesting to find out if the grid topologies impact the performance of the control algorithms.

4.3 | Simulation setup

In order to validate the effectiveness of the implemented algorithms, they are experimentally verified with a set of simulations performed on the RTS. The whole simulation setup is shown in Figure 12. The RTS used in this simulation setup is the OP 5600 from OPAL-RT technologies.

TABLE 2 Comparison of selected countries with respect to the different electrical parameters [44–47]

Parameters	Australia	China	Germany	Ghana	Latvia	Paraguay
Population, 2020 [Million]	25.5	1439.3	83.8	30.955	1.9	7.1
Electricity access [%]	100	100	100	85.17	100	99.3
Electricity generation, 2020 [TWh]	251.4	7623.7	567.3	19.71	5.8	49.8
RES share in production (including Hydro), 2020 [%]	24.9	29	44.9	32.34	61.1	100
Number of TSOs	5	2	4	1	1	1
Number of DSOs	15	2	883	3	10	1
Lowest transmission voltage [kV]	66	220	110	69	110	66
Distribution voltages [kV]	33; 22; 11; 6.6; 3.6	110; 10; 6	6; 10; 20; 33	33; 11	20; 10; 6	23
Household electricity price average, 2020 [$/kWh]	0.259	0.084	0.367	0.12	0.17	0.062
Allowed voltage range [%]	−5 to +10	±10	±10	±10	±10	±5
Distribution cables (predominantly)	Overhead	Underground	Underground	Overhead	Underground	Overhead
Drivers for grid expansion	PV, EV	RES, EV, rural electrification	RES, EV, Heat pumps	Rural electrification	PV, EV	Load
Voltage/power flow problem	Voltage	Both	Both	No	Voltage	Both
High load/ high infeed problem	Both	Both	Both	No	No	Load
Real-time measurements in MV/LV level	Yes	Yes (some)	Pilot projects	SCADA partial rollout	Pilot projects	Pilot projects
Remote-controlled switches for topology change	Pilot projects	Pilot projects	Pilot projects	No	Pilot projects	Pilot projects
OLTCs on MV/LV level	Remote and local operating	Rarely, locally controlled	Rarely, locally controlled	Rarely, locally controlled	Pilot projects	Pilot projects
(Typical) communication in the distribution level	Wired, sometimes wireless in LV	Mainly wireless	Wired, sometimes wireless in LV	SCADA exist up to 11 kV	Optical wired, sometimes wireless	Wired, SCADA system under development
Smart meter rollout	17.4% in 2021	Reached 99.57% in 2019	100% expected by 2032	Only high demand customers	100% expected by 2022	High demand customer
Typical grid topology in MV	Usually radial, rarely closed-ring	Usually radial, also closed-ring	Usually radial, also closed-ring	Urban: open-ring; rural: radial	Urban: open-ring; rural: radial	Usually radial
Representative grids in literature?	Yes [42]	No	Yes [43]	No	No	No

All the devices are connected to the same laboratory network. The client devices are responsible for communicating the measurements to the controller and transferring the P, Q setpoints to the controllable DERs in return. When the data model for each device is prepared and ready, the XML files are transferred to the individual measurement devices. All the grids are simulated with a time step of 250 μs. To simplify the test setup, only the controller IED is selected as the hardware device, while all the client IEDs and the representative grids are virtually simulated. This is done in order to reduce the number of physical measurements required in the test setup. The virtual IEDs are simulated within the RTS, such that the necessary measurements are sent from the RTS to the controller IED using UDP communication. The data configuration within the UDP signals is implemented similar to MMS, according to the IEC 61850 standards. The controller IED processes the received information using the implemented algorithms and sends out the DER P, Q setpoints to the respective client IEDs. If the OLTC tap is required, the command is sent back to the RTS using an electrical connection.

5 | REAL-TIME SIMULATION RESULTS

Since the loading and generation profiles of the real-world grids were not available, the loading and generation profiles were simulated to achieve voltage violations in the grid. Although the results of the experimental verification and the comparison between the implemented algorithms could be shown for every selected grid, the results of only three real-world grids are shown here due to space limitations. These are from China, Germany and Paraguay. They were chosen because the grids of China and Paraguay are more complex than the others. Also, the algorithms have to be investigated in the closed-ring grid of Germany to check if the grid topology has any impact on the algorithms.

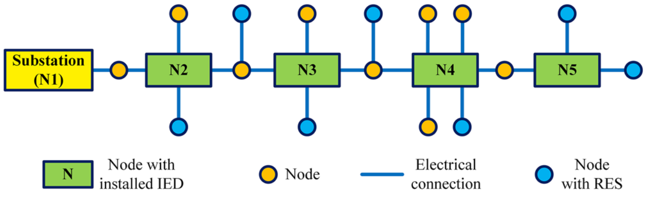

FIGURE 6 Representative real-world grid of Australia

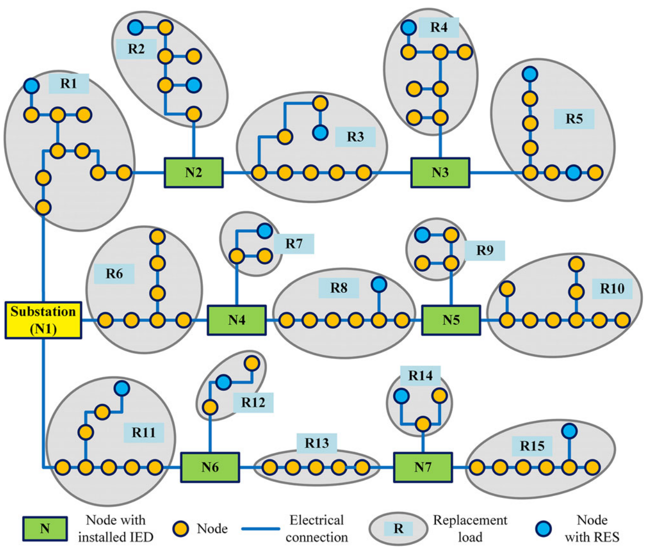

FIGURE 7 Representative real-world grid of China

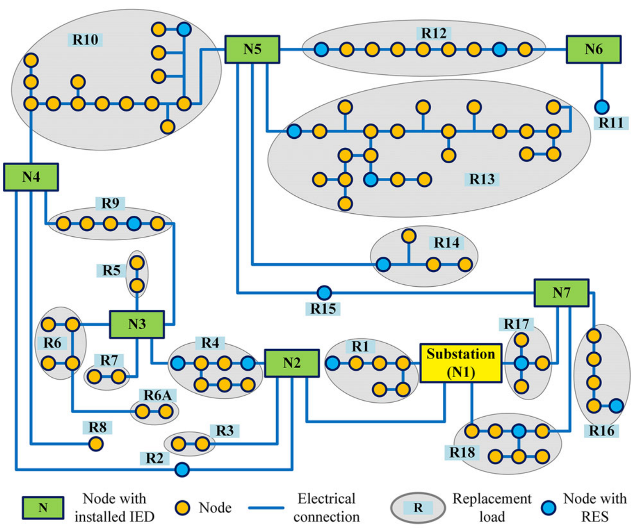

FIGURE 8 Representative real-world grid of Germany

5.1 | China

First, the results of the experimental verification in the representative grid of China are discussed. As shown in Figure 7, the grid has three feeders in each branch and each branch has a DER. The individual performance of the control algorithms,

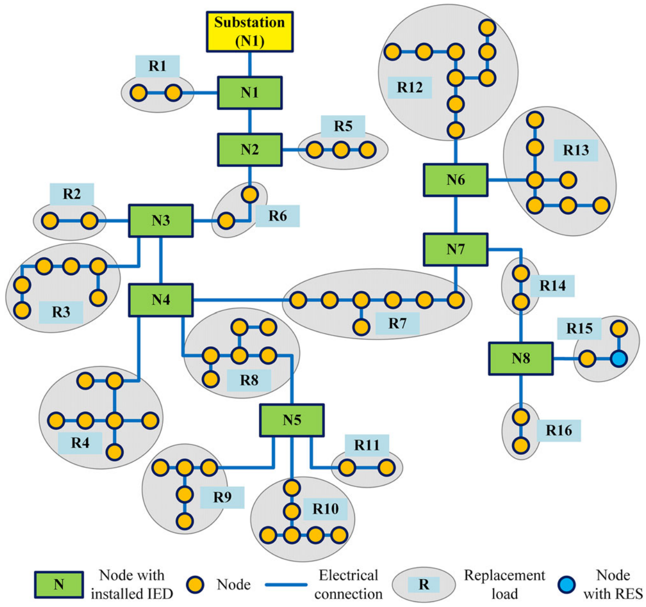

FIGURE 9 Representative real-world grid of Paraguay

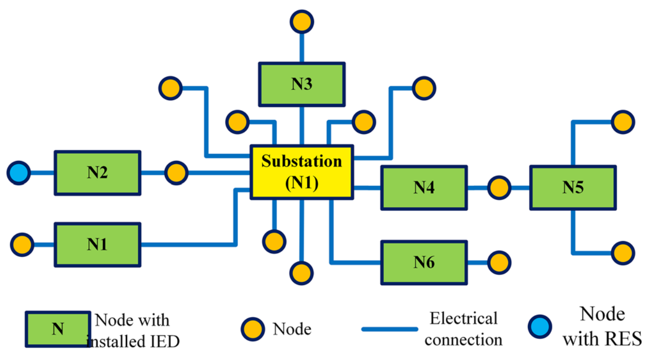

FIGURE 10 Representative real-world grid of Ghana

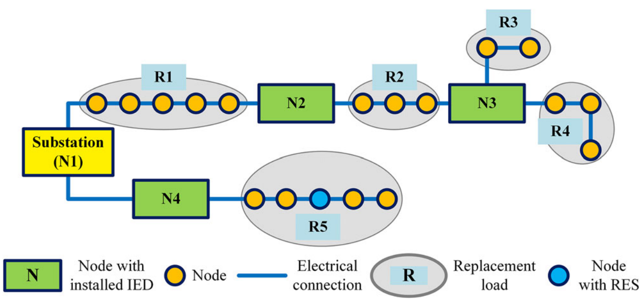

FIGURE 11 Representative real-world grid of Latvia

along with the maximum and minimum voltages during the control strategies, is sketched in Figure 13.

The available DERs are assumed to be controllable, and they are located inside the replacement nodes *R5*, *R10* and *R15*. Simulation scenarios were created to simulate a voltage violation in one of the feeders to test the implemented control functions. This way, the performance of the control algorithms could be investigated extensively. In addition, the case of no control is

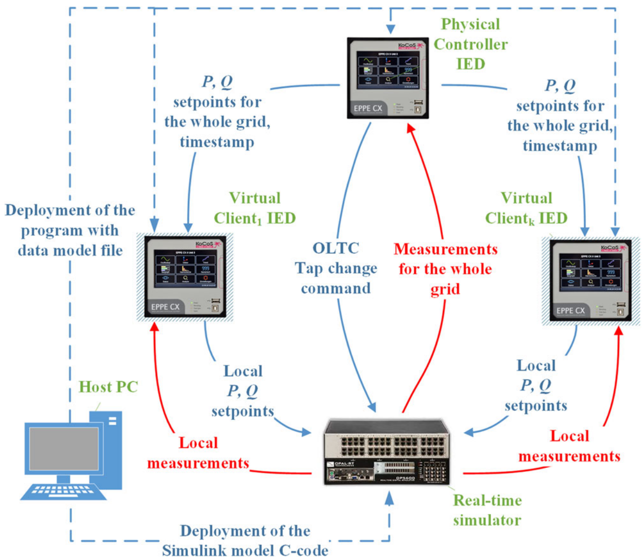

FIGURE 12 HiL simulation setup with the grids simulated on the RTS

also plotted in the graphs to indicate the grid performance without control. Figure 13a compares the performance of the CVC vs OPF algorithm. Figure 13b shows the Q setpoints at each of the three controllable DERs throughout the simulation. It can be seen that the Q control actions correspond to the required Q of the overall grid in response to the voltage control. The grid topology is very robust such that an OLTC stepping was not needed during the simulations.

The voltage limits for both CVC and OPF activation are set to ±4% from the nominal voltage. At $t \approx 120$ s, the first voltage violation occurs. In this case, the OPF reacts faster. During the subsequent breach around $t \approx 660\ s$, both under- and overvoltage problems are handled. Since the minimum voltage in the CVC reaches the activation limit of 0.96 pu earlier than the OPF, the CVC algorithm is activated earlier. As there is no differentiation between the DERs in the CVC implementation, the Q control at all generators is activated simultaneously.

In contrast, due to the network dynamics, the OPF reacts to the undervoltage first as it is detected earlier and later tries to handle the overvoltage by letting the DER at *R10* inject inductive Q. For all simulations, it is assumed that the full range of Q at ±100% of Q_{max} is available. The P setpoints of the DERs during the OPF algorithm are not shown here since no APC was required during the simulations. Because the objective function was configured for the OPF as per Equation (2), the Q setpoints calculated by the OPF change less over time than those computed using CVC. Note that this objective function does not penalise voltage quality, that is, any voltage that lies within the ±4% range is not considered by OPF.

5.2 | Paraguay

The following experiment deals with the 23 kV representative grid of Paraguay, shown previously in Figure 9. The available flexibilities are different from the previous case. Here, only one DER and an OLTC with 17 tap positions are available as flexibilities. The scenario for this experiment includes simulating only an under-voltage situation. The difference in this grid is that the voltage limits for control activation are set to only ±2%. This is because of the allowed voltage range of ±5%. The control values explained in Table 1 are divided in half to accommodate the voltage range. The controller triggers an OLTC stepping when the voltage violates the limit of ±3.5% at any point in the grid, according to Table 1. The results of the experimental verification of the control algorithms are shown in Figure 14. At t ≈ 12 s, the OPF algorithm fails to converge from the first time when trying to use only P, Q control of the DERs. It later converges after the OLTC is stepped up. The capabilities of the single controllable DER were not sufficient and the undervoltage situation was rectified with the use of OLTC. Later, at t ≈ 280 s, a similar situation is simulated and it can be seen that the OLTC steps up again. Because of the broader band of ±3.5%, the CVC algorithm behaves differently and steps up only once at t ≈ 160 s.

One could argue that OPF and CVC algorithms are unequal in such an implementation because OPF can already step at ±2%, while CVC needs to wait until the ±3.5% limit is reached. However, because of the stability issues in CVC, the Q control limit cannot be identical to the OLTC stepping, so the control parameters are set as close to each other as possible for both algorithms. It can be said that the OPF algorithm tries to keep the voltage at the best optimum according to the cost function, while the CVC algorithm keeps the voltage within limits, although without considering the costs.

5.3 | Germany

The following experimental setup deals with the 20 kV representative grid of Germany, shown previously in Figure 8. The dynamic simulation results are similar to those discussed before, where the control algorithms helped maintain the system voltage within limits. The change in the grid topology did not make any variation in the performance of the control algorithm. This means that the grid topology has little impact on the pertinence of the implemented control algorithms.

However, since the control parameters determine the performance of the control algorithms, it is also vital to choose the proper parameters. The parameters for both the control algorithms are varied according to Table 3.

TABLE 3 Change of the cost and control parameters

Control algorithm	Parameter	Original value	New value
OPF	c_P	$2e^3$	$1e^3$
	c_Q	$1e^2$	$2e^2$
CVC	K_p	3.5	0.9
	K_i	2	1.2
	K_d	0	0.1

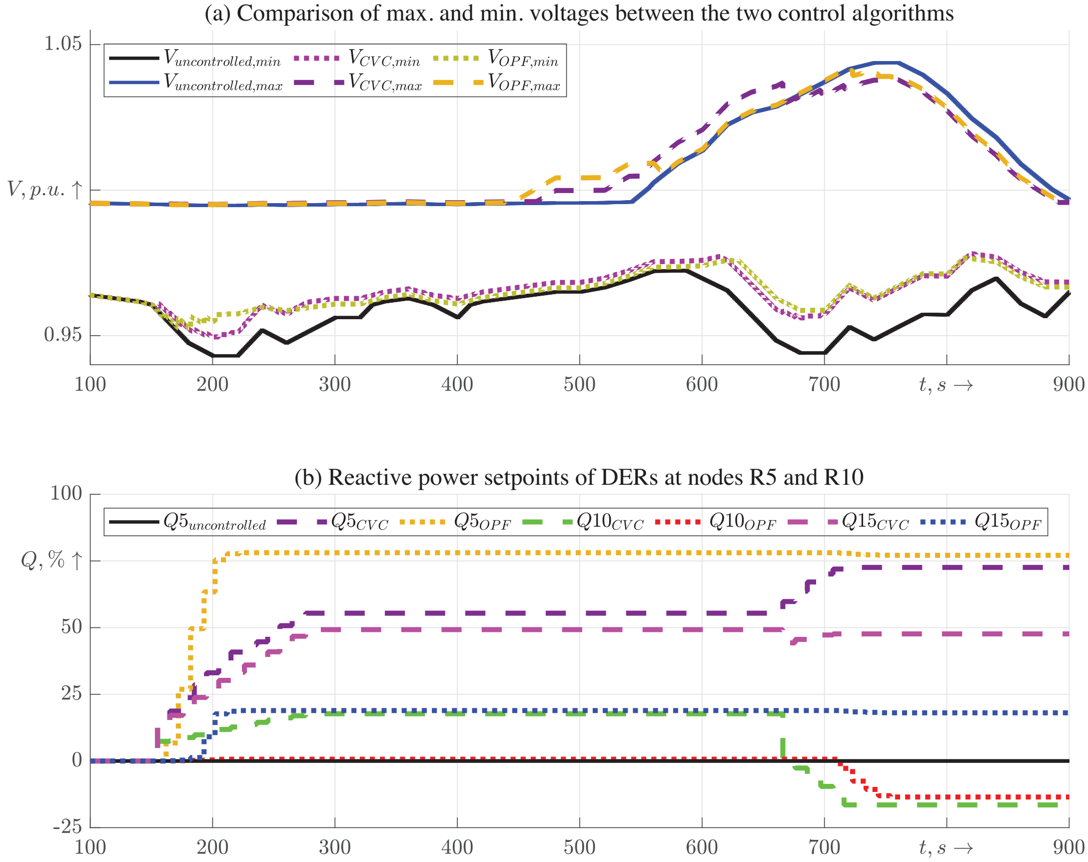

FIGURE 13 Time-domain results of the representative grid of China: CVC vs OPF algorithms, compared with the case of no control. The Q setpoints for the different DERs are also presented. Both the algorithms are executed every 30 seconds

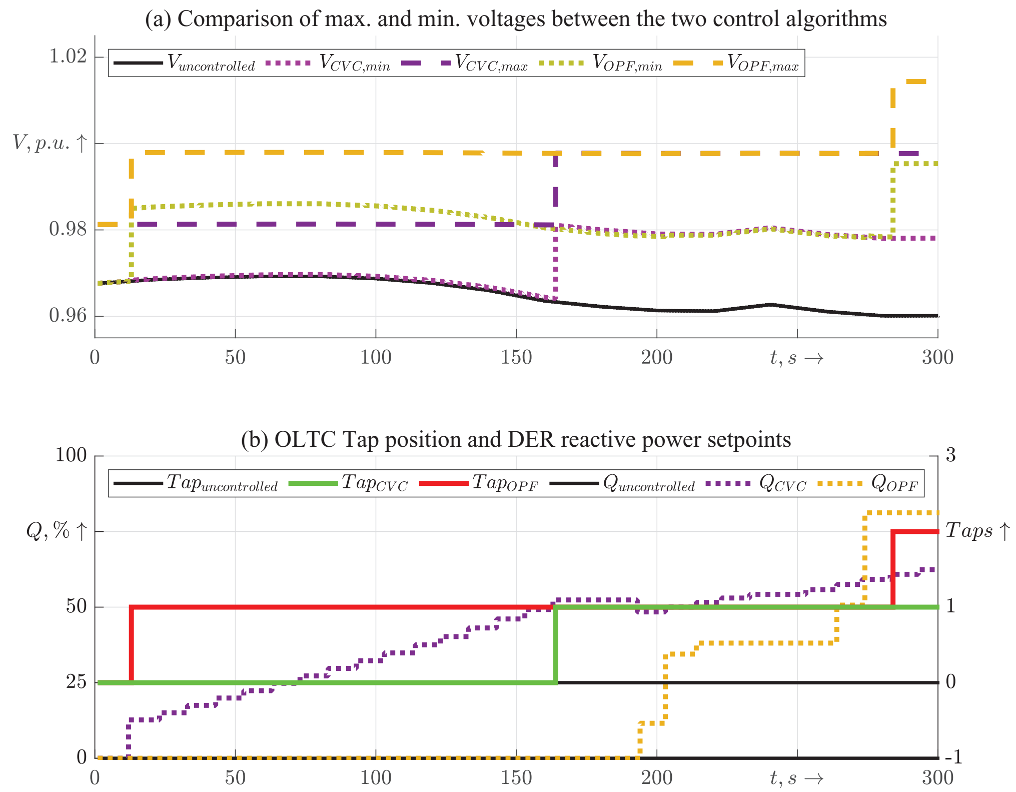

FIGURE 14 Time-domain results of the representative grid of Paraguay: CVC vs OPF algorithms, compared with the case of no control. The OLTC tapping and the DER Q setpoints are also presented. Both the algorithms are executed every 30 s

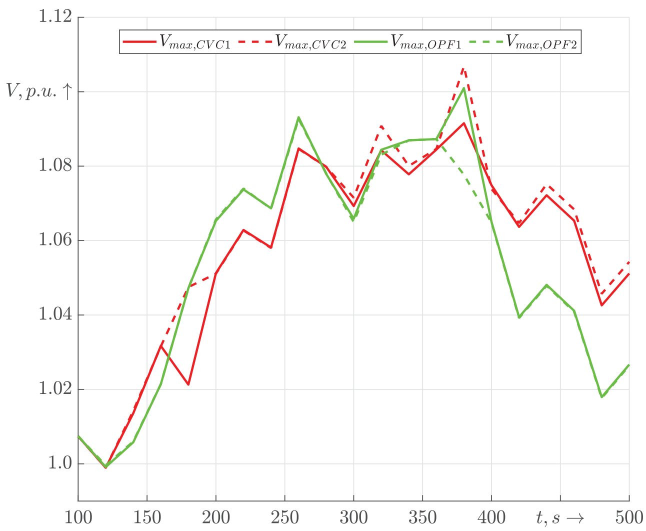

FIGURE 15 Comparison of maximum nodal voltages using different control parameters

To illustrate the significance of the control parameters in the system dynamics, the performances of the control algorithms have been compared against each other with varying control parameters and the results are shown in Figure 15.

As it can be seen, in addition to the performance changes between the two different control algorithms, there are also specific changes due to the variation of the control and cost parameters. The maximum nodal voltage in the grid is plotted for each case. The maximum nodal voltages with the original parameters are plotted in thick lines, while the dashed lines indicate those with the updated parameters. This proves that selecting the ideal control parameters is more important, irrespective of the grid itself. The parameters have to be chosen appropriately based on the individual characteristics of the particular grid under consideration. Selecting the proper control parameters for the PID controller can appear to be easy but is challenging in reality [48]. As proposed in [49], a self-adaptive PID controller could be used or by using optimisation algorithms, as presented in [50].

6 | CONCLUSION AND OUTLOOK

This work presents a solution for distribution automation implementation, which will be essential for future electrical grids, considering the enormous integration of DERs in the ADGs of the future. The proposed solution has an advantage due to the modular configuration using the IEC 61850 standards. It is hardware and vendor-independent and can easily be ported. The implemented control applications are non-device-specific and any additional protection or control algorithm from other vendors can be added at any point to the existing system, as long as the hardware prototype allows the integration.

The contribution of this paper is the modular configuration of the control algorithms using the IEC 61850 standards and the experimental verification in various representative real-world grids. The experimental verification of the proposed algorithms is done using HiL simulations and the results are discussed. The advantage of such an implementation is that new algorithms can be added to the existing framework, as long as it is configured using the IEC 61850 data models. This enables the user to potentially develop their own algorithms based on individual use cases. This means that a complete overhaul of the existing systems is not required. This way, it can be of enormous importance to the scientific community because the software becomes independent of the hardware provider.

While the OPF algorithm delivers the optimum grid state by making the best use of the available flexibilities, it is more complex to implement. The inherent challenge is that the optimisation could not converge for more complex networks when strict constraints are selected. In comparison, the CVC algorithm is much simpler to implement, although it has the challenge of identifying the best operating parameters for the PID controller. It does not need much computational power and is based on a simple PID controller. It can be argued that the PID controller is not very reliable and the performance depends on the parameter tuning. Having said that, such an algorithm could lower the hesitancy of the system operators to implement such an algorithm to control their field devices in the real world. When the advantages and limitations of both the algorithms are compared, it could be concluded that the CVC algorithm is suggested for smaller grids, where not many flexibilities are available and few critical nodes are identified for voltage or thermal violations. In the case of a much more complex grid structure with more flexibilities, the OPF is offered as the best possible solution strategy, as it involves finding the best-operating conditions for all the components involved.

Different dead bands are done to emulate real-world scenarios. This could have been avoided by using a standard 10% band. However, the real-world conditions might not be emulated rightly. It is right to say that the simulations have to be extended in order to test the algorithms at the regulatory limits, although the boundaries are scalable. The uncertainty of the DERs does not play a role in the performance of the implemented algorithms since they are based on real-time measurements. This could cause concern for algorithms involving predictions, such as Model Predictive Control (MPC).

When the performances of both the algorithms are compared against each other, the differences are not significant since the selected grids have only limited controllable DERs. However, the algorithms are scalable and are expected to provide promising results when applied to the distribution grids where more DERs are controllable in real-time. The practical realisation could take some time as the regulatory requirements should allow real-time control of the DERs. The implemented algorithms can be validated in reality only when the local grid policies allow such dynamic DER control.

Since the focus of the research is the modular implementation and not on the control algorithms themselves, two algorithms are exemplarily explained in this paper. Initially, the CVC algorithm was implemented. To overcome the shortcomings of the CVC implementation, OPF was implemented. Other control algorithms (e.g., MPC) are currently under implementation.

The communication among the various devices is done using TCP/UDP and work is in progress to establish communication using IEC 61850 MMS protocol. The transmission system is not considered in this particular implementation. A cross-voltage control strategy across MV-LV is currently under implementation. This information from the distribution grid could also be communicated to the control centre at the HV station. However, it is essential to figure out which values from the distribution grid will be sent to the control centre. Also, works are underway to use the synchronous machines and the power amplifiers (as DERs) available in the lab to validate the dynamic performance of the implemented algorithms.

ACKNOWLEDGEMENTS

This paper is based upon work in the project i-Automate (No. 03ET7561A), within the future-proof power grids initiative supported by the German Federal Ministry for Economic Affairs and Energy (BMWi).

CONFLICT OF INTEREST

None

DATA AVAILABILITY STATEMENT

The data that support the findings of this study are available from the corresponding author upon reasonable request.

REFERENCES

1. International Energy Agency (IEA): Renewable Energy Market Update - Outlook for 2021 and 2022 (2021)
2. International Energy Agency (IEA): Renewables 2020 - Analysis and Forecast to 2025 (2020)
3. German Federal Ministry for Economic Affairs and Energy: Renewable energy. https://www.bmwi.de/Redaktion/DE/Dossier/erneuerbare-energien.html. Accessed 28 December 2021
4. Voltage Characteristics of Electricity Supplied by Public Distribution Networks; EN 50160:2010. CENELAC European Committee for Electrotechnical Standardization, Brussels (2010)
5. Trilliant Holdings Inc.: Distribution automation (DA) - Trilliant. https://trilliant.com/applications/distribution-automation-da/. Accessed 28 December 2021
6. Zoho Corporation India: Power grid monitoring | RMS on Web-NMS IoT Platform. https://www.webnms.com/iot/smart-power-grid.html. Accessed 28 December 2021
7. Brenzikofer, A., et al.: GridBox pilot project: A platform for monitoring and active control of distribution grids. Comp. Sci. - Res. Develop. 32(1–2), 79–92 (2017)
8. Derviskadic, A., et al.: Design and Experimental Validation of an LTE-Based Synchrophasor Network in a Medium Voltage Distribution Grid. In: Power Systems Computation Conference (PSCC), pp. 1–7. IEEE, Piscataway (2018)
9. Kubis, A., Boller, M., Kemper, J., Uhlig, R., Stötzel, M., Stiegler, M.: Enhancing operational awareness of distribution system operators with a semi-autonomous intelligent grid control suite. In: CIRED 25th International Conference and Exhibition on Electricity Distribution, pp. 1–4. IEE, London (2019)
10. Carpita, M., Dassatti, A., Bozorg, M., Jaton, J., Reynaud, S., Mousavi, O.A.: Low voltage grid monitoring and control enhancement: The GridEye solution. In: International Conference on Clean Electrical Power (ICCEP), pp. 94–99. IEEE, Piscataway (2019)
11. Zimmerman, R.D., Murillo-Sánchez, C.E.: MATPOWER User's Manual, Version 7.0. https://matpower.org/docs/MATPOWER-manual-7.0.pdf. Accessed 28 December 2021
12. Bauernschmitt, B., Palaniappan, R., Hilbrich, D., Rehtanz, C.: Modular configurable and testable automation architecture for future active electrical energy grids. In: IEEE International Universities Power Engineering Conference (UPEC), pp. 1–6. IEEE, Piscataway (2018)
13. Palaniappan, R., Hilbrich, D., Bauernschmitt, B., Rehtanz, C.: Coordinated voltage regulation using distributed measurement acquisition devices with a real-time model of the Cigré low-voltage benchmark grid. IET Gener. Transm. Distrib. 13(5), 710–716 (2019)
14. KoCoS Messtechnik AG: EPPECX: Power quality measurement device. https://www.kocos.com/electrical-metrology/power-quality-analysers/eppe-power-quality-analysers/eppe-cx. Accessed 28 December 2021
15. Tuominen, J., Repo, S., Kulmala, A.: Comparison of the low voltage distribution network voltage control schemes. IEEE PES Innovative Smart Grid Technologies Conference Europe (ISGT-Europe), pp. 1–6. IEEE, Piscataway (2014)
16. Sun, H., et al.: Review of challenges and research opportunities for voltage control in smart grids. IEEE Trans. Power Syst. 34(4), 2790–2801 (2019)
17. Kraiczy, M., Al-Fakhri, L., Stetz, T., Braun, M.: Do It Locally: Local Voltage Support by Distributed Generation – A Management Summary. International Energy Agency, Paris (2017)
18. Fallahzadeh-Abarghouei, H., Nayeripour, M., Hasanvand, S., Waffenschmidt, E.: Online hierarchical and distributed method for voltage control in distribution smart grids. IET Gener. Transm. Distrib. 11(5), 1223–1232 (2017)
19. Robbins, B.A., Hadjicostis, C.N., Dominguez-Garcia, A.D.: A two-stage distributed architecture for voltage control in power distribution systems. IEEE Trans. Power Syst. 28(2), 1470–1482 (2013)
20. Antoniadou-Plytaria, K.E., Kouveliotis-Lysikatos, I.N., Georgilakis, P.S., Hatziargyriou, N.D.: Distributed and decentralized voltage control of smart distribution networks: Models, methods, and future research. IEEE Trans. Smart Grid 8(6), 2999–3008 (2017)
21. Kulmala, A., et al.: Hierarchical and distributed control concept for distribution network congestion management. IET Gener. Transm. Distrib. 11(3), 665–675 (2017)
22. Kulmala, A., Repo, S., Jarventausta, P.: Coordinated voltage control in distribution networks including several distributed energy resources. IEEE Trans. Smart Grid 5(4), 2010–2020 (2014)
23. Ahmed, M., Bhattarai, R., Hossain, S.J., Abdelrazek, S., Kamalasadan, S.: Coordinated voltage control strategy for voltage regulators and voltage source converters integrated distribution system. IEEE Trans. Ind. Appl. 55(4), 4235–4246 (2019)
24. Yang, G.Y., et al.: Analysis of Thevenin equivalent network of a distribution system for solar integration studies.In: 2012 3rd IEEE PES Innovative Smart Grid Technologies Europe (ISGT Europe), pp. 1–5. IEEE, Piscataway (2012)
25. Davoudi, M., Cecchi, V., Aguero, J.R.: Increasing penetration of distributed generation with meshed operation of distribution systems. In: North American Power Symposium (NAPS), pp. 1–6. IEEE, Piscataway (2014)
26. Liao, Y., Weng, Y., Rajagopal, R.: Urban distribution grid topology reconstruction via Lasso. In: IEEE Power and Energy Society General Meeting (PESGM), pp. 1–5. IEEE, Piscataway (2016)
27. Alzate, E.B., Li, Q., Xie, J.: A novel central voltage-control strategy for smart LV distribution networks. In: W. L. Woon, Z. Aung, S. Madnick (eds.) Lecture Notes in Computer Science, Data Analytics for Renewable Energy Integration, pp. 16–30. Springer International Publishing, Cham (2015)
28. Palaniappan, R., Molodchyk, O., Rehtanz, C.: Hardware Implementation of an OPF algorithm in a distribution network with decentralized measurements. CIRED Open Access J. 2020(1), 580–583 (2020)
29. Spalthoff, C., et al.: SimBench: Open source time series of power load, storage and generation for the simulation of electrical distribution grids. In: VDE International ETG Congress, pp. 1–6. VDE Verlag GmbH, Berlin (2019)
30. International Renewable Energy Agency (IRENA): Scaling Up Variable Renewable Power: The Role of Grid Codes. IRENA, New York (2016)
31. Mohseni, M., Islam, S.M.: Review of international grid codes for wind power integration: Diversity, technology and a case for global standard. Renew. Sustain. Energy Rev. 16, 3876–3890 (2012)

32. The World Bank - Energy Sector Management Assistance Program (ESMAP). Grid Integration Requirements for Variable Renewable Energy: ESMAP Technical Guide. World Bank, Washington DC (2019)
33. German Energy Agency: Energy Solutions Made in Germany: Innovative smart and sustainable energy technologies around the world. German Energy Agency, Berlin (2019)
34. Afandi, I., Agalgaonkar, A., Perera, S.: Market Structure for enabling volt/var control in australian distribution networks: A practical perspective. In: 19th International Conference on Harmonics and Quality of Power (ICHQP), pp. 1–6. IEEE, Piscataway (2020)
35. Western Power Distribution: Western power distribution - Projects. https://www.westernpower.co.uk/projects/network-equilibrium. Accessed 28 December 2021
36. VDE-AR-N 4110:2018-11: Technical Requirements for the connection and operation of customer installations to the medium voltage network (TAR medium voltage): Corrigendum 1. VDE FNN, Berlin (2020)
37. VDE-AR-N 4105:2011-08: Power Generation systems connected to the low-voltage distribution network: Technical minimum requirements for the connection to and parallel operation with low-voltage distribution networks. VDE FNN, Berlin (2011)
38. IEEE Standard for Interconnection and Interoperability of Distributed Energy Resources with Associated Electric Power Systems Interfaces, IEEE 1547–2018. IEEE Standards Coordinating Committee 21 (2018)
39. Implementation of the Network Code on Requirements for Grid Connection of Generators. European Commission, Brussels (2021)
40. German Federal Ministry for Economic Affairs and Energy: Innovation durch Forschung: Erneuerbare Energien und Energieeffizienz: Projekte und Ergebnisse der Forschungsförderung 2018 (2019)
41. Wikimedia Commons: CIA WorldFactBook - Political world.png. Accessed 18 June 2021
42. CSIRO Data Access Portal: Representative Australian electricity feeders with load and solar generation profiles. https://data.csiro.au/collections/collection/CI15331v001. Accessed 28 December 2021
43. SimBench: Benchmark grids. https://simbench.de/de/. Accessed 28 December 2021
44. Our World in Data: Electricity generation. https://ourworldindata.org/grapher/share-electricity-renewables. Accessed 28 December 2021
45. United Nations Department of Economic and Social Affairs: World population prospects - Population division. https://population.un.org/wpp/Download/Standard/Population/. Accessed 28 December 2021
46. Küfeoğlu, S., Pollitt, M., Anaya, K.: Electric power distribution in the World: Today and Tomorrow. Cambridge Energy Policy Research Group Working Paper in Economics (2018)
47. GlobalPetrolPrices: Electricity prices around the world. https://www.globalpetrolprices.com/electricity_prices/. Accessed 28 December 2021
48. Ang, H., Chong, G., Li, Y.: PID control system analysis, design, and technology. IEEE Trans. Control Syst. Technol. 13(4), 559–576 (2005)
49. Yan, X., Sun, J., Li, Y., Qi, J., Pan, Y.: Self-adaptive tuning of fuzzy PID control of PV grid-connected inverter. In: 6th International Conference on Fuzzy Systems and Knowledge Discovery (FSKD), pp. 160–162. IEEE, Piscataway (2009)
50. Roni, M.H.K., Rana, M.S.: Optimized PID control scheme for three phase micro-grid system. In: 2nd International Conference on Robotics, Electrical and Signal Processing Techniques (ICREST), pp. 77–80. IEEE, Piscataway (2021)

How to cite this article: Palaniappan, R., Molodchyk, O., Shariati-Sarcheshmeh, M., Asmah, M. W., Liu, J., Schlichtherle, T., Richter, F., Kwofie, E. A., Festner, D. R., Blanco, G., Mutule, A., Borscevskis, O., Rafaat, S. S., Li, Y., Häger, U., Rehtanz, C.: Experimental verification of smart grid control functions on international grids using a real-time simulator. IET Gener. Transm. Distrib. 16, 2747–2760 (2022). https://doi.org/10.1049/gtd2.12486